

Preparation of machinable cordierite/mica composite by low-temperature sintering

Seichi Taruta*, Takeshi Hayashi, Kunio Kitajima

Department of Chemistry and Materials Engineering, Faculty of Engineering, Shinshu University, 4-17-1, Wakasato, Nagano-shi, Nagano, 380-8553, Japan

Received 8 September 2003; received in revised form 30 October 2003; accepted 8 November 2003

Abstract

In order to fabricate machinable cordierite/mica composite at low temperatures, the mica-composition glass powder was mixed with the conventional magnesia, alumina and silica powders which are raw materials of cordierite, compacted and fired in a sealed platinum container. By the addition of the 40 mass% mica-composition glass powder, machinable cordierite/mica composite was obtained. The machinability was caused by the interlocking microstructure of mica developed in the composite. In the firing process, mica crystallized at about 730 °C, cordierite was suddenly formed at 1050–1100 °C and the densification progressed markedly at 1000–1100 °C. The formation and sintering of cordierite were strongly promoted by a small amount of gaseous fluorine and/or fluorides. It was considered that fluorine and fluorides such as AlF_3 evaporated from the mica-composition glass at > 800 °C and gaseous HF was formed in the sealed platinum container by the reaction of fluorine with water evaporated from the glass.

© 2003 Elsevier Ltd. All rights reserved.

Keywords: Composites; Cordierite; Machinability; Mica; Powders-solid state reaction; Silicates; Sintering

1. Introduction

Cordierite ceramics have many valuable properties. They are well known as materials used for honeycomb-shaped catalyst carriers in automobile exhaust systems, utilizing their low thermal expansion coefficient and high chemical stability.^{1–13} Recently, they are expected as substrate materials for integrated circuit boards and semiconductor packaging because of their low dielectric constant in high-frequency regions and high electric resistivity.^{2–4,6–8,11,13–18} However, it is difficult to make dense cordierite ceramics with the high mechanical strength because the difference between densification and decomposition temperatures of cordierite is very small in a firing process.^{1–3,5–7,9,12,13,16,18,19} Therefore, many studies on the powder synthesis and the sintering of cordierite have been reported.^{1–19} By the sol-gel method using complex-alkoxide¹⁵ and the emulsion processing,¹³ dense α -cordierite ceramics are obtained at low temperatures of 1050–1100 °C while α -cordierite

ceramics are densified at 1200–1350 °C in many cases. Moreover, the densification temperatures are lowered by the addition of B_2O_3 ,^{15,17} P_2O_5 ¹⁸ and Bi_2O_3 .^{4,12}

On the other hand, the cordierite ceramics are difficult to be machined by the ordinary metal tools due to their hardness and brittleness as well as many other ceramics. The improvement of the machinability is very effective in the fabrication of complex shape ceramics, precision machining, machining efficiency and reduction of machining cost. Machinable $\text{Si}_3\text{N}_4/\text{h-BN}$ ^{20–23} and $\text{Al}_2\text{O}_3/\text{h-BN}$ ²⁴ composites which utilize the machinability of h-BN, and machinable $\text{Al}_2\text{O}_3/\text{LaPO}_4$,^{23,25,26} mullite/ LaPO_4 ,²⁵ $\text{ZrO}_2/\text{LaPO}_4$ ^{25,27} and $\text{ZrO}_2/\text{CePO}_4$ ²⁵ composites which utilize the weak interface between oxides and phosphates, have been reported. However, machinable ceramics/mica sintered composites are not obtained while mica glass-ceramics were well known machinable ceramics. We could fabricate spinel/mica composites by the sintering of spinel and mica-composition glass powder mixtures and the crystallization of mica from the powder mixtures.^{28–30} Moreover, we found that using magnesia and alumina powders as raw materials of spinel, the composites were densified at lower temperatures.³¹ However, such spinel/mica

* Corresponding author. Tel.: +81-26-269-5416; fax: +81-26-269-5424.

E-mail address: staruta@gipwc.shinshu-u.ac.jp (S. Taruta).

composites did not show the machinability because the mica was not sufficient to form interlocking micro-structure.

In this study, our aim was to fabricate machinable cordierite/mica composites at low temperatures. So the mica-composition glass powder was mixed with the conventional magnesia, alumina and silica powders which are raw materials of cordierite. We expected that in the firing process, after crystallization of mica, the formation and sintering of cordierite would be promoted by the liquid phase resulting from the melt of the residual glass. The reaction and sintering of the powder mixtures and some properties of obtained cordierite/mica composites were investigated.

2. Experimental procedure

The mica-composition (fluorophlogopite: $\text{KMg}_3\text{Al-Si}_3\text{O}_{10}\text{F}_2$) glass powder was prepared by the melting method, of which the details are given elsewhere.^{28–31} It was mixed with magnesia (MJ-30, Iwatani Chemicals, Japan, average particle size of 0.36 μm), alumina (AES-12, Sumitomo Chemicals, Japan, average particle size of 0.52 μm) and amorphous silica (SO-C2, Admatechs, Japan, particle size: 0.4–0.6 μm) powders by a ball milling. The mixing ratio of the magnesia, alumina and amorphous silica powders corresponded to a stoichiometric cordierite composition ($2\text{MgO} \cdot 2\text{Al}_2\text{O}_3 \cdot 5\text{SiO}_2$) and the additions of the mica-composition glass powder were 0, 10, 20 and 40 mass%. The four specimens are called here the 0, 10, 20 and 40%, respectively. The powder mixtures were calcined at 600 °C for 1 h, passed through a 100-mesh sieve, compacted by a cold-isostatic pressing at 98 MPa and fired in a sealed platinum container.

Crystalline phases in the specimens were determined using an X-ray diffractometry (XRD). The bulk densities were measured by the Archimedes method. The polished and chemically etched surfaces of the sintered specimens were observed by a scanning electron microscopy (SEM). The three point bending strength, Vickers hardness, fracture toughness and thermal expansion coefficient were measured. The machinability was qualitatively evaluated using a bench-drilling machine. The drill made of hard metal was used and the rotational frequency was 620 rpm.

3. Results and discussion

3.1. Phase change and sintering

XRD patterns of the 40% specimen are shown in Fig. 1. Mica was separated at <1050 °C and α -cordierite was suddenly formed at 1100 °C. A small amount of

spinel remained even at 1250 °C. Similar phase changes were observed in the 10% and 20% specimens while mica was not detected for the 10% specimen. In the 0% specimen, α -cordierite appeared at 1350 °C. In many studies,^{1–3,6–9,11,13–18} μ -cordierite is formed and it transforms to α -cordierite at higher temperatures. However, μ -cordierite was not observed in this study, which is characteristic of this system. Even if μ -cordierite was formed, it would exist in very short term. Bulk densities of each specimen are shown in Fig. 2. The 10% specimen had a large bulk density even at 1050 °C, but the main crystalline phases were not cordierite. When

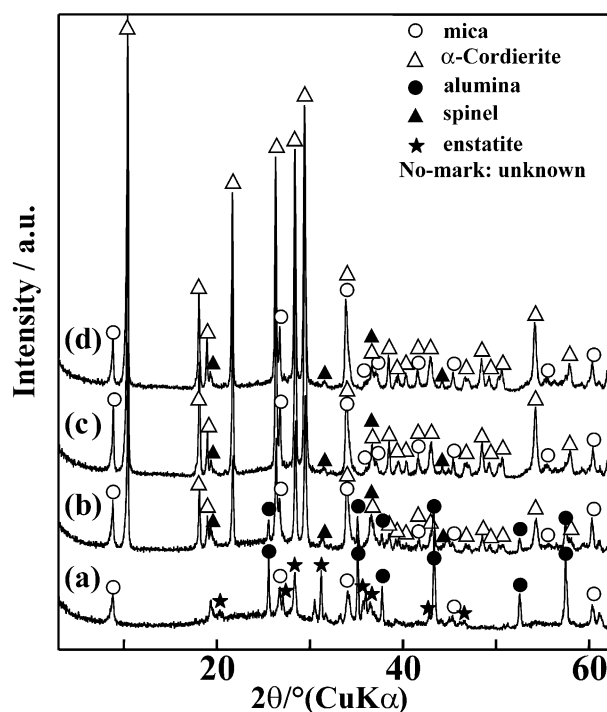


Fig. 1. XRD patterns of the 40% specimen fired at (a) 1050 °C, (b) 1100 °C, (c) 1150 °C and (d) 1250 °C for 2 h.

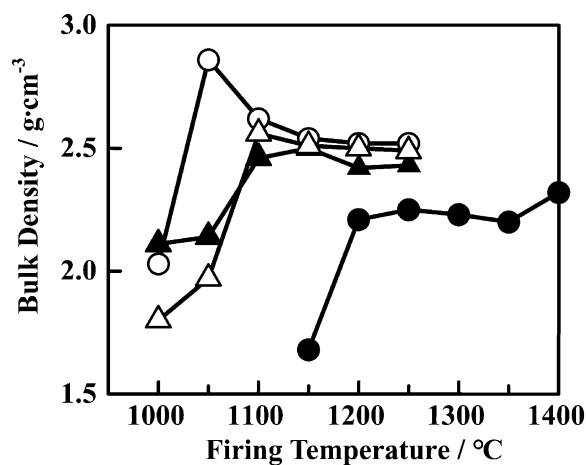


Fig. 2. Bulk densities of sintered specimens. (●): 0%, (○): 10%, (▲): 20% and (△): 40%.

the cordierite was formed at 1100 °C, the bulk density decreased because the theoretical density of cordierite (2.499 g/cm³) is lower than those of alumina (3.987 g/cm³) and enstatite (3.208 g/cm³). On the other hand, the bulk densities of the 20% and 40% specimens were much lower than that of the 10% specimen at 1050 °C. Much addition of the mica-composition glass powder caused the crystallization of mica while it impeded the densification. This means that the densification of the 20% and 40% specimens was impeded by mica. However, the 20% and 40% specimens became as dense as the 10% specimen at 1100 °C and their relative densities reached 95–97% at 1150 °C. SEM photographs of

the 40% specimen fired at 1050–1200 °C for 2 h are shown in Fig. 3. At 1050 °C, isotropic grains with size under 1 µm might correspond to alumina, enstatite and unknown crystals. Flake-like crystals which are characteristic of mica were not observed despite its detection by XRD. The mica crystals should be very fine. At 1100 °C, the microstructure became dense and flake-like mica crystals with size under 1 µm were observed. The size of isotropic grains almost did not change and was <1 µm though the formation reaction of cordierite occurred. At 1200 °C, the cordierite grains grew to 1–3 µm, being smaller than those of the 10% and 20% specimens (see Fig. 4). This indicates that the grain growth of cordierite was impeded by mica. The finer isotropic grains observed in the 10%, 20% and 40% specimens must be alumina, spinel and unknown crystals, which are shown in the arrows in Fig. 3 and Fig. 4. They were difficult to react and form cordierite because they were placed inside the cordierite grains. Therefore, most remain unchanged even at higher temperatures. Flake-like mica crystals in the 40% specimen grew to 2–3 µm and formed the interlocking microstructure.

Above results indicate that the addition of the mica-composition glass was very effective in the formation and sintering of cordierite. As additive agents for such

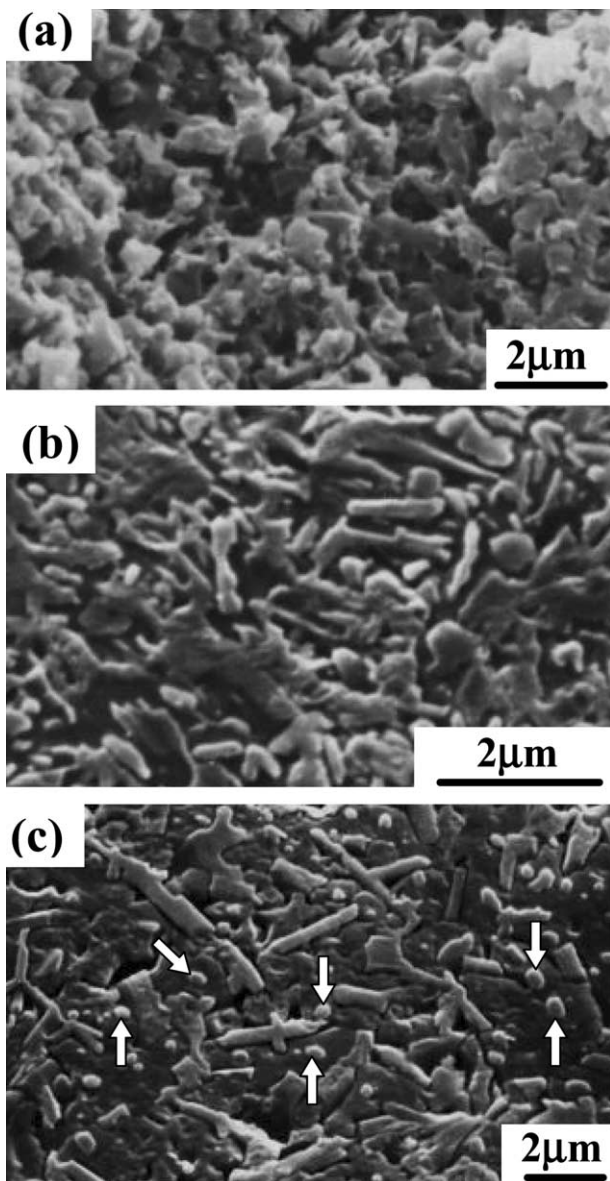


Fig. 3. SEM photographs of the 40% specimen fired at (a) 1050 °C, (b) 1100 °C and (c) 1200 °C. (a) is the fracture surface. (b) and (c) are polished and chemically etched surfaces. The finer isotropic grains shown in arrows in (c) might be spinel and unknown crystals.

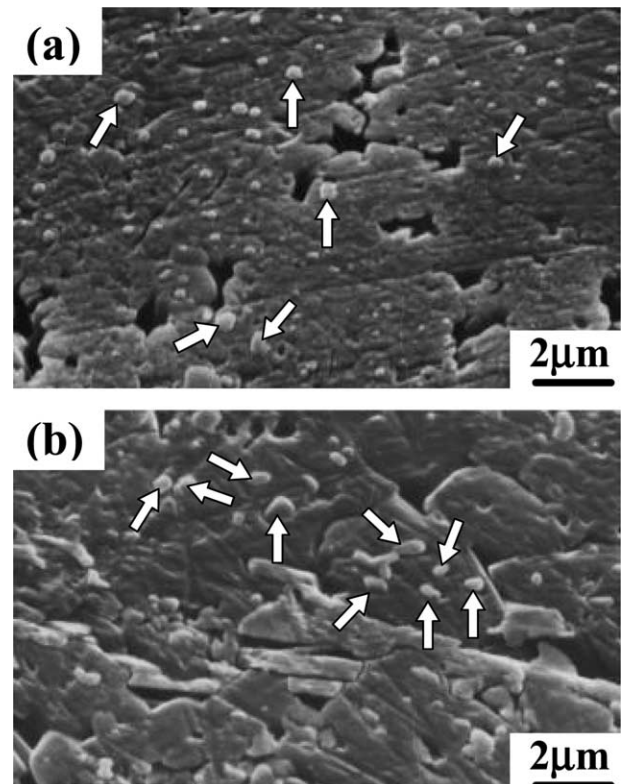


Fig. 4. SEM photographs of the polished and chemically etched surfaces of the (a) 10% and (b) 20% specimens fired at 1200 °C for 2 h. The finer isotropic grains shown in arrows might be alumina, spinel and unknown crystals.

formation and sintering, B_2O_3 ,^{15,17} P_2O_5 ¹⁸ and Bi_2O_3 ^{4,12} were reported. Among these, Bi_2O_3 acts as flux. In this study, a differential thermal analysis (DTA) of the mica-composition glass powder shows that mica crystallized at about 730 °C and the residual glassy phase melted at about 965 °C, such as shown in Fig. 5. Therefore, we supposed that the liquid phase resulting from the melt of the residual glassy phase should promote the reaction and sintering. However, because the reaction almost did not depend on added amount of the glass and much addition impeded the densification, following experiments were attempted; the powder compact of the 0% specimen was fired together with a powder compact of the mica-composition glass in a sealed platinum container, assuring that both compacts did not contact each other. The XRD patterns of the 0% specimen are shown in Fig. 6. Cordierite was formed at 1150 °C and the relative density of the sintered compact was about 97%. Thus, gas phases evaporated from the mica-composition glass seem to play an important role in the reaction and sintering, while the role of liquid phase is minor. The gas phases were analyzed using a temperature programmed desorption (TPD type V, Rigaku, Japan) mass spectrometer. The change of the total ionic current with an increase in

temperature and the mass spectrums at 422 °C and 1092 °C are shown in Fig. 7. It is clear from the change of the total ionic current that gas phases evaporated from the mica-composition glass at temperatures under 700 °C and above 800 °C. As the gas phases evaporated at <700 °C, H_2O , CO and CO_2 were identified from the spectrums at 157 °C, 345 °C and 422 °C. The weight loss

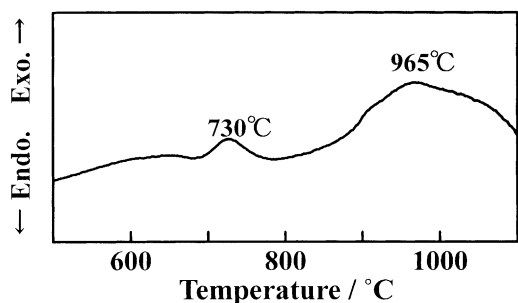


Fig. 5. DTA curve of the mica-composition glass powder.

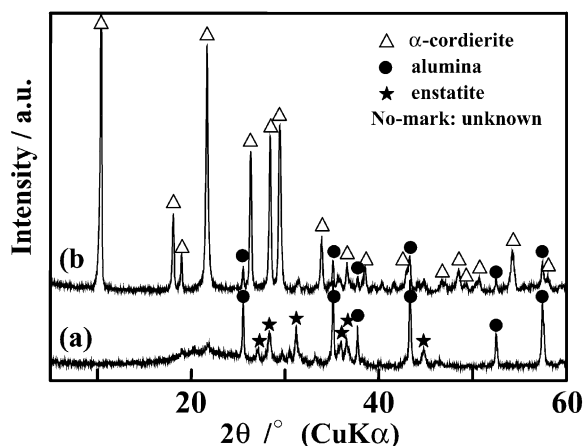


Fig. 6. XRD patterns of the 0% specimen fired at (a) 1100 °C and (b) 1150 °C for 2 h together with the mica-composition glass powder compact in the sealed platinum container.

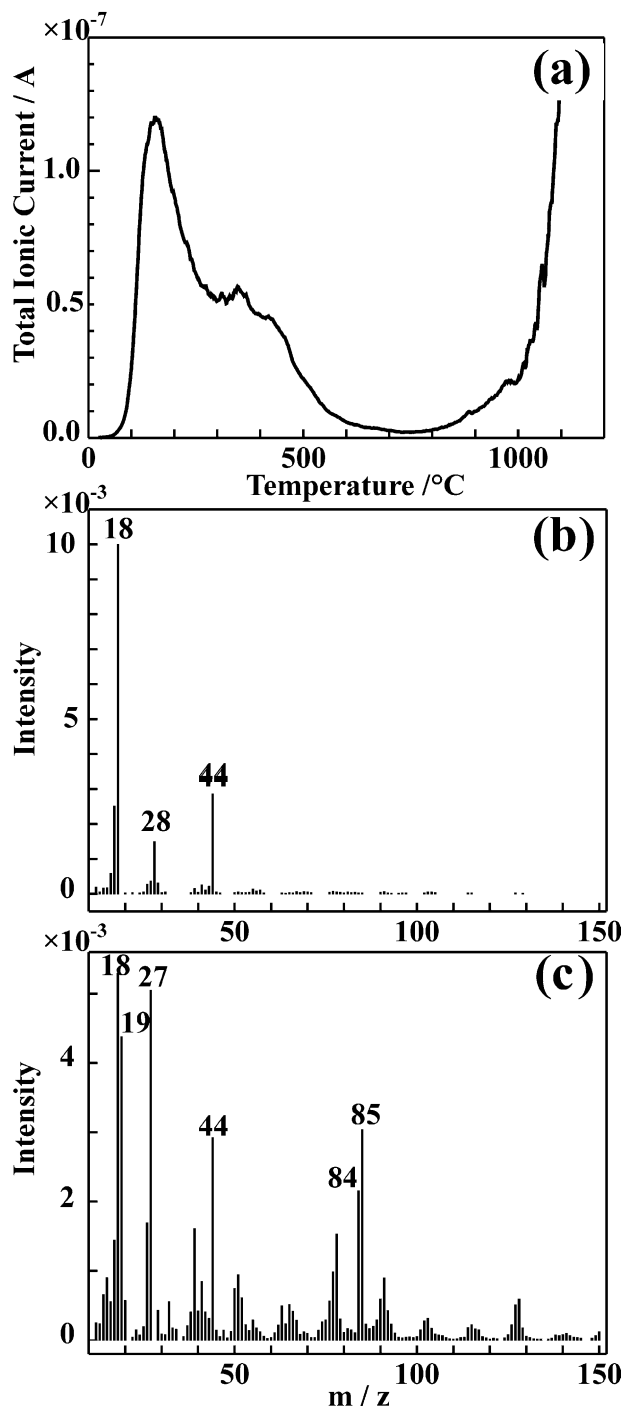


Fig. 7. (a) Change of the total ionic current of gas evaporated from the mica-composition glass powder upon heating; mass spectra obtained at (b) 422 °C and (c) 1092 °C are also shown.

Table 1
Some properties of each specimen fired at 1200 °C for 2 h

Specimen	Thermal expansion coefficient ^b /K ⁻¹	Bending strength/MPa	Vickers hardness/GPa	Fracture toughness/MPa·m ^{1/2}
0% ^a	1.95×10^{-6}			
10%	2.17×10^{-6}	96.8 ± 8.3	7.4 ± 0.4	2.4 ± 0.1
20%	2.62×10^{-6}	131.8 ± 8.7	7.1 ± 0.5	2.4 ± 0.1
40%	3.35×10^{-6}	142.7 ± 3.9	4.7 ± 0.5	2.9 ± 0.2

^a This specimen was fired at 1400 °C for 2 h.

^b Temperature range from RT to 927 °C.

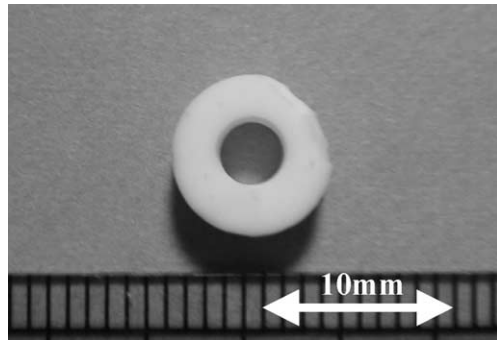


Fig. 8. Photograph of drilling test of the 40% specimen fired at 1200 °C for 2 h.

of the mica-composition glass was 2.0% at <700 °C. The identification of the gas phases evaporated at >800 °C was difficult and not completed from the mass spectrum measured at 1092 °C. However, F (mass number: 19), Al (mass number: 27) and AlF₃ (mass number: 84) were confirmed. This indicates that fluorine and fluorides such as AlF₃ evaporated from the mica-composition glass at >800 °C. The weight loss of the mica-composition glass was 0.3% at 800–1200 °C. Moreover, in the sealed platinum container fluorine would react with water vapor and form the gaseous HF. These results mean that a very small amount of gaseous fluorine and/or fluorides such as HF and AlF₃ played a significant role in the formation and sintering of cordierite.

3.2. Mechanical and thermal properties

The photograph of drilling test for the 40% specimen sintered at 1200 °C for 2 h are shown in Fig. 8. The drill penetrated easily into the 40% specimen with the thickness of 2–3 mm and fatal large chippings were not observed. Thus, a machinable cordierite/mica composite was obtained in this study. This machinability was caused by the interlocking microstructure of mica in the composite, known as “house-of-cards structure”. The mechanical and thermal properties of each specimen sintered at 1200 °C for 2 h are shown in Table 1. The bending strength increased by enhancing the additive amount of the glass. In addition, the pore size tended to decrease with an increase in the additive amount of the

glass (Figs. 3 and 4). These indicate that the crystallization of mica decreased the size of fracture origin. The bending strength of the 40% specimen was relatively high when compared with reported strength of cordierite (70–180 MPa),^{3,10,11,15,19} while B₂O₃ doped cordierite ceramics showed maximum bending strengths of 190 MPa¹⁵ or >200 MPa.¹⁷ However, the Vickers hardness of the 40% specimen dropped markedly due to the formation of the interlocking microstructure of mica. The thermal expansion coefficient increased with an increase in the additive amount of the glass. The 40% specimen had a value which is half of that of alumina ($7 \times 10^{-6}/^{\circ}\text{C}$) and is very close to that of Si ($3.5 \times 10^{-6}/^{\circ}\text{C}$). Thus, obtained cordierite/mica composite can be expected to be utilized as substrate materials for integrated circuit boards and also as thermal shock resistance ceramics with machinability. Moreover, it can be produced at low temperatures and at low machining cost.

4. Conclusions

By adding mica-composition glass powder to the conventional magnesia, alumina and silica powders which are raw materials of cordierite, dense cordierite/mica compositions were obtained at low temperatures of 1100–1200 °C. In the firing process, mica crystallized at about 730 °C, while cordierite was suddenly formed at 1050–1100 °C. The densification progressed markedly at 1000–1100 °C. The formation and sintering of cordierite were strongly promoted by a small amount of gaseous fluorine and/or fluorides such as HF and AlF₃. It was considered that fluorine and fluorides such as AlF₃ evaporated from the mica-composition glass at >800 °C and gaseous HF was formed in the sealed platinum container by the reaction of fluorine with water evaporated from the glass.

Machinable cordierite/mica composite was obtained by the addition of 40 mass% mica-composition glass powder, which could be machined by the conventional hard metallic tool. In addition, it showed relatively high bending strength and almost the same thermal expansion coefficient as silicon. However, its Vickers hardness was lower than that of cordierite ceramics.

Acknowledgements

The authors would like to thank Rigaku Ltd. for the experimental support of the vapor phase analysis using TPD and to thank Iwatani Chemicals Ltd., Sumitomo Chemicals Ltd. and Admatechs Ltd. for the support of magnesia, alumina and amorphous silica powders, respectively.

References

1. Suzuki, H., Ota, K. and Saito, H., Preparation of cordierite ceramics from metal alkoxides (Part 1)—preparation and characterization of the powder. *J. Ceram. Soc. Japan (Yogyo-Kyokai-Shi)*, 1987, **95**, 163–169.
2. Suzuki, H., Ota, K. and Saito, H., Preparation of cordierite ceramics from metal alkoxides (Part 1)—sintering. *J. Ceram. Soc. Japan (Yogyo-Kyokai-Shi)*, 1987, **95**, 170–175.
3. Suzuki, H., Ota, K. and Saito, H., Mechanical properties of alkoxy-derived cordierite ceramics. *J. Mater. Sci.*, 1988, **23**, 1534–1538.
4. Dupon, R. W., McConville, R. L., Musolf, D. J., Tanous, A. C. and Thompson, M. S., Preparation of cordierite below °C via bismuth oxide flux. *J. Am. Ceram. Soc.*, 1990, **1000**, 73 335–339.
5. Kazakos, A. M., Komarneni, S. and Roy, R., Sol-gel processing of cordierite: effect of seeding and optimization of heat treatment. *J. Mater. Res.*, 1990, **5**, 1095–1103.
6. Kikuchi, N., Sei, T., Tsuchiya, T., Hayashi, S. and Hayamizu, K., Preparation of cordierite ceramics by the sol-gel process and their properties. *J. Ceram. Soc. Japan*, 1993, **101**, 824–829.
7. Sumi, K., Kobayashi, Y. and Kato, E., Synthesis and sintering of cordierite from kaolinite and basic magnesium carbonate. *J. Ceram. Soc. Japan*, 1998, **106**, 89–93.
8. Sumi, K., Kobayashi, Y. and Kato, E., Synthesis and sintering of cordierite from ultrafine particles of magnesium hydroxide and kaolinite. *J. Am. Ceram. Soc.*, 1998, **81**, 1029–1032.
9. Lee, S.-J. and Kriven, W. M., Crystallization and densification of nano-size amorphous cordierite powder prepared by a PVA solution-polymerization route. *J. Am. Ceram. Soc.*, 1998, **81**, 2605–2612.
10. Nakahara, M., Kondo, Y., Nakagawa, Z. and Hamano, K., Effects of calcination and grinding of starting kaolin material on microstructure and physical properties of cordierite ceramics. *J. Ceram. Soc. Japan*, 1999, **107**, 1118–1121.
11. Kobayashi, Y., Sumi, K. and Kato, E., Preparation of dense cordierite ceramics from magnesium compounds and kaolinite without additives. *Ceram. Int.*, 2000, **26**, 739–743.
12. Malachevsky, M. T., Fiscina, J. E. and Esparza, D. A., Preparation of synthetic cordierite by solid-state reaction via bismuth oxide flux. *J. Am. Ceram. Soc.*, 2001, **84**, 1575–1577.
13. Chan, K. C., Ovenstone, J. and Ponton, C. B., Emulsion processing as a novel rout to cordierite. *J. Mater. Sci.*, 2002, **37**, 971–976.
14. Okuyama, M., Fukui, T. and Sakurai, C., Effects of complex precursors on alkoxide-derived cordierite powder. *J. Am. Ceram. Soc.*, 1992, **75**, 153–160.
15. Okuyama, M., Fukui, T. and Sakurai, C., Phase transformation and mechanical properties of B₂O₃-doped cordierite derived from complex-alkoxide. *J. Mater. Sci.*, 1993, **28**, 4465–4470.
16. Oh, J. R., Imai, H. and Hirashima, H., Effect of Al/Si ratio on crystallization of cordierite ceramics prepared by the sol-gel method. *J. Ceram. Soc. Japan*, 1997, **105**, 43–47.
17. Sumi, K., Kobayashi, Y. and Kato, E., Low-temperature fabrication of cordierite ceramics from kaolinite and magnesium hydroxide with boron oxide additions. *J. Am. Ceram. Soc.*, 1999, **82**, 783–785.
18. Mei, S., Yang, J. and Ferreira, J. M. F., Microstructural evolution in sol-gel derived P₂O₅-doped cordierite powders. *J. Eur. Ceram. Soc.*, 2000, **20**, 2191–2197.
19. Nakahara, M., Kondo, Y. and Hamano, K., Effect of particle size of powders ground by ball milling on densification of cordierite ceramics. *J. Ceram. Soc. Japan*, 1999, **107**, 308–312.
20. Wang, R., Pan, W., Jiang, M., Chen, J. and Luo, Y., Investigation of the physical and mechanical properties of hot-pressed machinable Si₃N₄/h-BN composites and FGM. *Mater. Sci. Eng.*, 2002, **B90**, 261–268.
21. Kusunose, T., Sekino, T., Choa, Y. H. and Niihara, K., Fabrication and microstructure of silicon nitride/boron nitride nanocomposites. *J. Am. Ceram. Soc.*, 2002, **85**, 2678–2688.
22. Kusunose, T., Sekino, T., Choa, Y.-H. and Niihara, K., Machinability of silicon nitride/boron nitride nanocomposites. *J. Am. Ceram. Soc.*, 2002, **85**, 2689–2695.
23. Wang, R., Pan, W., Chen, J., Fang, M., Jiang, M. and Luo, Y., Graded machinable Si₃N₄/h-BN and Al₂O₃/LaPO₄ ceramic composite. *Mater. and Design*, 2002, **23**, 565–570.
24. Li, Y., Qiao, G. and Jin, Z., Machinable Al₂O₃/BN composite ceramics with strong mechanical properties. *Mater. Res. Bull.*, 2002, **37**, 1401–1409.
25. Davis, J. B., Marshall, D. B., Housley, R. M. and Morgan, P. E. D., Machinable ceramics containing rare-earth phosphates. *J. Am. Ceram. Soc.*, 1998, **81**, 2169–2175.
26. Min, W., Miyahara, D., Yokoi, K., Yamaguchi, T., Daimon, K., Hikichi, Y., Matsubara, T. and Ota, T., Thermal and mechanical properties of sintered LaPO₄-Al₂O₃ composites. *Mater. Res. Bull.*, 2001, **36**, 936–945.
27. Min, W., Daimon, K., Matsubara, T. and Hikichi, Y., Thermal and mechanical properties of sintered machinable LaPO₄-ZrO₂ composites. *Mater. Res. Bull.*, 2002, **37**, 1107–1115.
28. Suzuki, S. S., Taruta, S. and Takusagawa, N., Sintering and microstructure of alumina/mica and spinel/mica composites. *Korean J. Ceram*, 1998, **4**, 363–367.
29. Suzuki, S. S., Taruta, S. and Takusagawa, N., Influence of the amount of fluorophlogopite-composition glass on the microstructure and the mechanical properties of spinel/mica composites. *J. Ceram. Soc. Japan*, 2000, **108**, 548–553.
30. Suzuki, S. S., Taruta, S., Kitajima, K. and Takusagawa, N., Mechanical properties of spinel/mica composites. *J. Ceram. Soc. Japan*, 2000, **108**, 1079–1084.
31. Taruta, S., Yonekura, H., Suzuki, S. S., Kitajima, K. and Takusagawa, N., Sintering and contact damage of spinel/mica composites prepared from alumina, magnesia and mica-composition glass powder mixtures. *J. Ceram. Soc. Japan*, 2002, **110**, 208–210.